Magnetic polarons in weakly doped high-T_c superconductors

E. M. Hankiewicz,* R. Buczko, and Z. Wilamowski
Institute of Physics, Polish Academy of Sciences, al. Lotników 32/46, 02-668 Warsaw, Poland
(Received 30 August 2001; revised manuscript received 18 June 2002; published 23 August 2002)

The formation of magnetic polarons in an antiferromagnetic medium is studied numerically in wide range of parameters with special attention to high-T_c superconductors. We consider a Hamiltonian describing d-d exchange interactions between d spins of a finite Heisenberg antiferromagnet, p-d interactions between a conducting hole p, and d spins, as well as kinetic energy of hole. The decoupling of orbital and spin degrees of freedom allows us to consider the spin Hamiltonian and kinetic energy separately. The spin Hamiltonian is solved exactly with use of the Lanczos method of diagonalization. We conclude that p-d exchange interaction favors magnetic polarons localized on one site of the antiferromagnet. Adding the kinetic energy does not change essentially the phase diagram of magnetic polarons formation. For parameters relevant for high-T_c superconductors either a polaron localized on one lattice cell or a small ferron form. However, we find that the contribution of magnetic and phonon terms in the formation of a polaron in weakly doped high-T_c materials can be comparable.

DOI: 10.1103/PhysRevB.66.064521 PACS number(s): 74.20.−z, 74.72.−h, 71.38.−k

I. INTRODUCTION

The role of phonon and spin exchange in the formation of polarons and bipolarons in CuO_2 based high-T_c materials has been a matter of extensive discussion from the very moment high-T_c superconductors were discovered. Experimental observations of the anomalous isotope effect[1,2] could indicate the role of phonon interactions in the formation of the superconducting state. On the other hand, angle-resolved photoemission spectroscopy[3] (ARPES), transport,[4] and tunneling microscopy measurements[5] show d symmetry of the order parameter indicating an important role of exchange. Although some authors underline the role of both mechanisms,[6] the solution of full Hamiltonian is complicated and these contributions are usually calculated separately.

The concept of the phonon polaron was introduced by Pekar[7] and Fröhlich.[8,9] It was adopted to high-T_c superconductors by Alexandrov and Mott.[10] Its energy was estimated to be as fraction of eV. Moreover, it was proposed[11] that the narrowing of the d-electron band by the polaron effect and the formation of phonon bipolarons increases the critical temperature to $T_c \approx 100$ K. However, because of the dominant contribution of d symmetry to the order parameter, exchange interactions are the most often considered ones recently. Modeling of such interactions is difficult because it is necessary to include the role of conducting (p) holes as well as localized (d) electrons.

In the case of weak p-d couplings, a linear response of the antiferromagnet (AF) can be assumed. Hence a phenomenological model of magnetic susceptibility introduced by Millis, Monien, Pines[12] (MMP) can be used. Zhang and Rice,[13] in turn, describe the case of strong hybridization between the $3d$ states of Cu and $2p$ states of O. When the hybridization is much greater than the kinetic energy of the carriers, it is possible to limit the description to the ground singlet state, and in such a case a one band model can be used. This model (called t-J) is at present the most often used to describe the cuprate superconductors (for a review, see Ref. 14). Unfortunately, different techniques of approximations lead sometimes to contradictory solutions of t-J, as it is in the case of the stripe formation.[15,16] In the framework of the t-J model, the formation of the spin polaron was extensively investigated by many authors.[17–22]

However, the spin-fermion model,[23–30] which treats separately the spin of p-carrier and d-localized spins, seems to be the most appropriate for the case of intermediate p-d coupling typical for high-T_c superconductors. Most papers treat the p-d interaction as a Kondo exchange. Such an approach shows the tendency of cuprates to stripe phase formation[23] or d-wave pairing.[26,25] Recently, Bała *et al.*[29,30] extended the spin-fermion model starting from the three band Hubbard model. In their model, p-d coupling is more complicated than the Kondo one because some exchange couplings between the Cu ion and two neighboring oxygen atoms appear. The model, based on self-consistent Born approximation (SCBA), describes the formation of magnetic polaron[29,30] and identifies all the spectrum of energy states of the Zhang-Rice polaron[30] in angular resolved ultraviolet photoemission spectroscopy (ARUPS) experiments.[31] However, a comparison of SCBA and exact diagonalization techniques for spin-fermion model has not been carried out yet.

The present paper reports on systematic calculations of a simple spin-fermion model with an exact diagonalization technique for a spin Hamiltonian. Since the spin-fermion model allows us to investigate the cases of strong and intermediate p-d coupling, this approach broadens the possible range of solutions. Thus a comparison of the phonon and magnetic contributions to the formation of a polaron in weakly doped high-T_c superconductors for a wide range of parameters is possible. The exchange interactions are calculated strictly while the phonon contribution is evaluated in the framework of the Fröhlich theory.[8–10]

In Sec. II, we describe the Hamiltonian and the method of finding the ground and excited states of the system. In Sec. III, the exchange spin interactions are analyzed. In Sec. IV, we analyze the phase diagram of different magnetic polarons. In Sec. V, we compare contributions from phonon and magnetic polarons. A summary is given in Sec. VI.

II. MODEL

We study a system of d localized spins and the mobile p-like hole treating all spins quantum mechanically. In particular, we think of d spins within the quantum antiferromagnet (AF) model, i.e., none of the Néel sublattices are chosen *a priori*. We consider finite one- (1D) and two-dimensional (2D) AF clusters with different boundary conditions. The spin interactions in the system and the kinetic energy T of the p hole is described by the Hamiltonian

$$H=2J_{dd}\sum_{\langle i,j\rangle}\mathbf{S}_i\mathbf{S}_j+\frac{1}{2}J_{pd}\sum_{i,\alpha,\beta}\mathbf{S}_i c^{+}_{i\alpha}\boldsymbol{\sigma}_{\alpha\beta}c_{i\beta}+t_{ij}\sum_{i,j,\alpha}c^{+}_{i\alpha}c_{j\alpha}, \tag{1}$$

where $\mathbf{S}_i$ is the effective spin of the nine core d electrons ($3d^9$), the summation is taken over the pairs of nearest-neighbor (NN) d spins $\langle i,j\rangle$, $\boldsymbol{\sigma}_{\alpha\beta}$ are the Pauli matrices of the p hole with spin $s=1/2$,J_{pd} is the Kondo parameter normalized to the volume of elementary cell, J_{dd} is the exchange integral between d-d spins, t_{ij} is the hopping matrix element to the neighbor, $c^{+}_{i\alpha}$, $c_{i\alpha}$ are the operators of creation and annihilation of a hole on the ith site with spin projection α. We look for the eigenstates of the Hamiltonian (1) in the form

$$\Psi\cdot X_S. \tag{2}$$

Here X_S is the spin state vector of the system. The orbital wave vector Ψ in the space of the single hole occupation at AF sites $i=1,\ldots,N$ takes a form

$$\Psi=\sum_{i}^{N}\varphi(i)u_i, \tag{3}$$

where $u_i=|0,0,\ldots,1,0,0\cdots\rangle$ is the occupation vector of the hole at ith site, $\varphi(i)$ is the corresponding probability amplitude and N is the number of spins of AF cluster. To solve the eigenproblem we use the variational method with Ψ as the trial function. It is normalized by the condition $\Sigma_{i=1}^{N}|\varphi(i)|^2=1$. Equation (2) allows for separate diagonalization of the kinetic and exchange terms of Hamiltonian (1),

$$H'=\langle\Psi|H|\Psi\rangle=T+H_s. \tag{4}$$

T does not depend on the spin state and can be evaluated from the probability amplitude of the carrier $\varphi(i)$:

$$T=z|t_1|-2|t_1|\sum_{\langle i,j\rangle}\varphi(i)\varphi(j), \tag{5}$$

if only the hopping to NN, t_1 is considered, and z is the number of NN's. The term $z|t_1|$ provides $T=0$ for fully delocalized states. Diagonalization of the spin Hamiltonian,

$$H_s=2J_{dd}\sum_{\langle i,j\rangle}\mathbf{S}_i\mathbf{S}_j+\sum_{i}j_{pd}(i)\mathbf{S}_i\mathbf{s}, \tag{6}$$

yields the exchange energy. Here $\mathbf{s}$ is the p-spin operator and the p-d exchange integrals are given by

$$j_{pd}(i)=J_{pd}|\varphi(i)|^2. \tag{7}$$

To compare the results for 1D and 2D clusters, we introduce $J'_{pd}=J_{pd}/(2zJ_{dd})$, which describes the ratio of p-d to d-d coupling normalized by the number of AF bonds, $2z$. Moreover, $J'_{pd}\ll 1$ describes the range of a weak p-d coupling, while $J'_{pd}>1$ that of a strong p-d one, independent of the dimensionality.

We use the Lanczos method of diagonalization of the Hamiltonian (6). Diagonalization of matrices for AF cluster with $N\leqslant 20$ is possible with the personal computer.

The main goal of the paper is a detailed study of quantum coupling between spins within the polaron in an AF medium. We focus our analysis on the gain of the spin-exchange energy,

$$E_{ex}=E^0_{dd}-(E_{dd}+E_{pd}), \tag{8}$$

where E^0_{dd} is energy of the ground state of the unperturbed AF (when $J_{pd}=0$) and $E_{dd}+E_{pd}$ is the total exchange energy of the system when the carrier is coupled to AF. In this way, we analyze the zero-temperature case only. We found that for a weak p-d exchange the gain E_{ex} is a half of the p-d coupling energy, $E_{ex}=-E_{pd}/2$.

We describe the spin structure and formation of the antiferromagnetic polarons (AFP) by means of correlators between d spins $\langle\mathbf{S}_i\mathbf{S}_j\rangle$ as well as between the p and d spins $\langle\mathbf{s}\mathbf{S}_i\rangle$,

$$M_L(i)=\langle\mathbf{s}\mathbf{S}_i\rangle=\langle X_S|\mathbf{s}\mathbf{S}_i|X_S\rangle, \tag{9}$$

where $M_L(i)$ has a sense of local magnetization of d spins ''seen'' by a carrier.

The assumption that the wave function can be described by Eq. (2) is simplified. In general, the total wave function is at least the linear combination of the pair of such functions localized on two Néel sublattices. This problem is discussed in Sec. III G.

Hamiltonian (1) does not contain a phonon term. In general, the coupling of the carrier to the lattice polarization and the exchange interactions act together to form the polaron. This issue is addressed in Sec. V.

III. SPIN STRUCTURE OF MAGNETIC POLARONS

We examine various types of trial functions φ. Depending on the size and shape of the carrier distribution, $|\varphi|^2$ (Fig. 1), as well as on the value of exchange constants (Fig. 2), various types of magnetic polarons with very different spin structures can be found.

(i) Large AFP: Its size r_p is much greater than the lattice constant a_0 and the AF correlation range ξ. Thus it can be described within the model of a linear response. For large polarons, the magnetization $M_L(i)$ becomes proportional to the local carrier density.[12]

(ii) Medium AFP: Its size r_p is comparable or smaller than ξ, but bigger than $\sim 0.4a_0$ (see Fig. 1). Here the carrier interacts with a few local spins inducing staggered polarization.

(iii) Small AFP: It is localized within a single elementary cell. For very strong p-d coupling it corresponds to the Zhang-Rice (ZR) polaron.

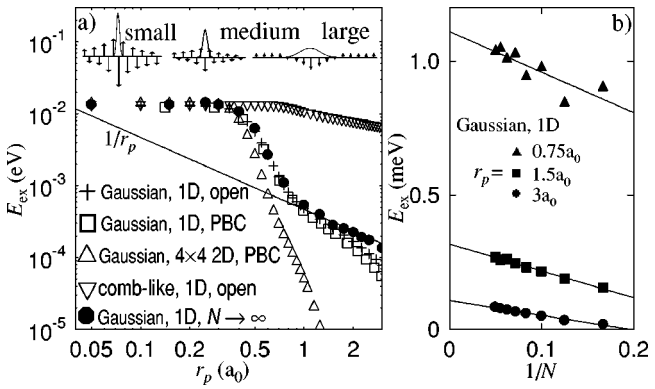

FIG. 1. (a) E_{ex} as a function of polaron size for various trial functions and AF clusters with $N=16$. At the top, arrows show the correlators between p and d spins, $M_L(i)$, for different AFP's while solid curves depict trial functions. For a large AFP the arrow size is multiplied 30 times. (b) Extrapolation of E_{ex} to infinite 1D AF for selected r_p.

(iv) Ferron: It forms when the p-d exchange is strong enough to break AF bonds and to induce a homogeneous magnetic moment.[32]

(v) Comblike AFP: It is the case when the carrier is distributed on one Néel sublattice only. The staggered polarization is the dominant response of AF.[25,33]

The clear difference between AFP's of different sizes is seen in Fig. 1(a), where the energy gain E_{ex} is plotted as a function of r_p. Gaussian trial function $|\varphi(i)|^2\propto\exp[-(\mathbf{r}_i-\mathbf{r}_0)^2/(2r_p^2)]$, where $\mathbf{r}_i-\mathbf{r}_0$ is the distance from central spin, was used to calculate most of the data. Down triangles depict results calculated using another trial function, and they describe a comblike AFP, discussed in Sec. III E. In Fig. 1(a), the calculations were done for $J'_{pd}=1/4$. Here the small AFP corresponds to $r_p\lesssim 0.4a_0$, medium to $0.4a_0\lesssim r_p\lesssim a_0$, and large to $r_p\gtrsim a_0$.

Figure 1(b) shows that $E_{ex}\propto 1/N$ where N is a chain length. It makes the extrapolation to an infinite N possible. Extrapolated $E_{ex}(N\to\infty)$ are plotted by full circles in Fig. 1(a). A comparison of numerical data for finite and extrapolated to infinity AF clusters shows that we calculate small, medium, and large AFP in 1D with good accuracy. We find the same for small and medium AFP in the 2D case. However, because of computational limitations, we cannot carry out the full extrapolation for large AFP's in two dimensions. A comparison of numerical results for open chains and chains with periodic boundary conditions (PBC's) shows that the use of PBC's does not lead to an improvement of the convergence of numerical results. It is in part an effect of the Ψ normalization and of specific properties of the dangling spins at the cluster border.

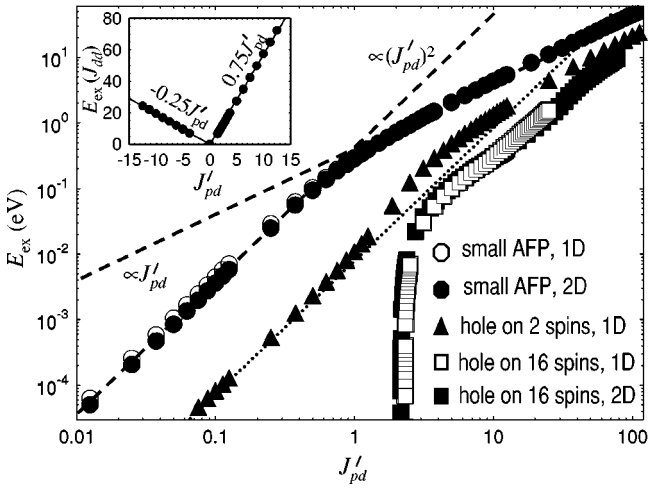

FIG. 2. E_{ex} for different AFP's and AF clusters of $N=16$ spins as a function of J'_{pd}. The inset shows $E_{ex}(J'_{pd})$ for a small AFP.

A. Large AFP

Figure 1 shows the decrease of the E_{ex} as $1/r_p$ for 1D large AFP's i.e., for $r_p\gtrsim a_0$. Below we compare the numerical $E_{ex}(1/r_p)$ with an analytical solution in which the magnetic susceptibility of AF is described by two phenomenological parameters. The analytical solution gives a better description of large AFP's while the comparison with the numerical results allows us to explain the physical meaning of the phenomenological parameters.

For simplicity in the analytical approximation, we use an exponential distribution of carrier density, $|\varphi(\mathbf{r}')|^2=[1/(2r_p)]\exp(-|\mathbf{r}'-\mathbf{r}_0|/r_p)$, which does not change the results qualitatively. We assume that the susceptibility can be described by the phenomenological formula introduced in the MMP model,[12] $\chi(\mathbf{q})=\chi_{q_0}/[1+(\mathbf{q}-\mathbf{q}_0)^2\xi^2]$, where $\mathbf{q}$ is the wave vector and $q_0=\pi/a_0$ corresponds to the staggered magnetization. The phenomenological parameters χ_{q_0} and ξ describe the staggered magnetic susceptibility and the spin correlation length, respectively. An effective field acting on d spins is $H_{eff}(\mathbf{r}')=[J_{pd}a_0/(4g\mu_B r_p)]\exp(-|\mathbf{r}'-\mathbf{r}_0|/r_p)$. Within the approximation of linear response and continuous media, induced magnetization has a form $M(\mathbf{r})=\int d\mathbf{r}'\chi(\mathbf{r}-\mathbf{r}')H_{eff}(\mathbf{r}')$ at the point $\mathbf{r}$. Thus this approach accounts for the nonlocal effects of correlated systems but neglects the atomic structure of AF. For large AFP's, i.e., for $r_p\gg\xi$, $M(\mathbf{r})$ takes the form

$$M(\mathbf{r})=\frac{J_{pd}a_0\chi_{q_0}}{16\pi^2 g\mu_B\xi^2}\frac{1}{q_0^2 r_p}\exp\left(-\frac{|\mathbf{r}-\mathbf{r}_0|}{r_p}\right). \qquad (10)$$

Thus $M(\mathbf{r})$ induced by a large AFP is smooth and has a spatial dependence of the carrier density. The icon in Fig. 1 shows numerically calculated correlators between the p-spin $\mathbf{s}$ and local spins $\mathbf{S}_i$ for a large AFP. One can see that for a large AFP the induced $M_L(i)$ is also smooth and proportional to $|\varphi(i)|^2$. In that sense the analytical solution is equivalent to the numerical one.

E_{ex} has a simple form in the analytical approach:

$$E_{ex}=\frac{(J_{pd}a_0)^2\chi_{q_0}}{256\pi^2(g\mu_B)^2\xi^2 q_0^2 r_p}. \qquad (11)$$

The absolute value of E_{ex} and its dependence on either the d-d exchange or on ξ cannot be calculated from Eq. (11).

However, Fig. 1(b) shows the important numerical result, that E_{ex} is almost independent on chain length N. Hence, if one attributes ξ to N, Eq. (11) leads to the conclusion that $\chi_{q_0} \propto \xi^2/J_{dd}$ for a large 1D AFP.

For 2D large polaron, we find a faster, $1/r_p^2$ decrease of E_{ex} as compared to the 1D case. This leads to the important conclusion about the existence of large AFP in two dimensions when the total energy E_{tot} is considered. Because both $E_{ex}, T \propto 1/r_p^2$, two scenarios are possible: (i) no polaron forms when $T \gtrsim E_{ex}$, or, in the opposite case, (ii) the minimum of E_{tot} occurs for $r_p \to 0$ (see also Fig. 6), i.e., beyond the definition of large AFP.

B. Medium AFP

Figure 1 shows that for $r_p \lesssim a_0$, E_{ex} does not follow the $1/r_p$ dependence. E_{ex} increases rapidly as r_p decreases for one dimension and even sharper for two dimensions as compared to $1/r_p$ dependence. This dramatic increase of E_{ex} indicates a tendency to localization of medium AFP's. At the same time, a qualitative change of $M_L(i)$ induced in the AF medium takes place. As it is shown by icons in Fig. 1, $M_L(i)$ is smooth for $r_p \gtrsim a_0$ while for $r_p \lesssim a_0$ it becomes staggered.

Figure 2 shows another important result concerning medium polarons. When charge is distributed only on two d spins and $J'_{pd} \lesssim 1$, $E_{ex} \propto J'^2_{pd}$. However, for $J'_{pd} \gtrsim 1$ a more complex behavior occurs. The AF bonds broke and a ferron forms (see Sec. III D).

C. Small AFP

Figure 1 shows that when the polaron size becomes comparable to the size of the elementary cell ($r_p \lesssim 0.4a_0$), E_{ex} saturates. This result weakly depends on either the size of AF cluster or boundary conditions. $M_L(i)$ induced by the small AFP is staggered similarly to the case of medium AFP as shown by icons in Fig. 1.

A dependence of E_{ex} on J'_{pd} for small polarons is shown by circles in Fig. 2. There is no considerable difference between 1D and 2D cases. For a small $J'_{pd} \lesssim 1$ $E_{ex} \propto J'^2_{pd}$ while for $J'_{pd} \gtrsim 1$ it becomes linear. Now we show that this crossover corresponds to dramatic changes in spin structure. Figures 3(a) and (c) present correlators between different spins of the system: the carrier spin $\mathbf{s}$ and AF spin $\mathbf{S}_0$ on which the carrier is localized, between $\mathbf{s}$ and d spins $\mathbf{S}_i$, and between $\mathbf{S}_0$ and $\mathbf{S}_i$. Figure 3(b) shows z components $\mathbf{s}_z$ and $\mathbf{S}_{0z}$ of the p spin and d spin, respectively, and the sum of all d spins $\Sigma_i \mathbf{S}_{iz}$. The z direction is set by an infinitesimally small magnetic field. A number of important conclusions emerge from these data. First, for $J'_{pd} \lesssim 1$ the magnetization of the d spin on which carrier is localized $\langle \mathbf{sS}_0 \rangle$ increases linearly and saturates at $\langle \mathbf{sS}_0 \rangle = -3/4$ in the same range of J'_{pd} for which $E_{ex} \propto J'_{pd}$ [cf. Figs. 2 and 3(a)]. That means compensation of the d spin by the spin of a carrier for large J'_{pd}. Second, as one can see from icons in Fig. 3(a) as well as from Fig. 3(c), the magnetization induced by small polaron changes with J'_{pd}. $M_L(i)$ is staggered for a weak p-d coupling while both magnetization of d spins (besides $\mathbf{S}_0$) and $\langle \mathbf{S}_0 \mathbf{S}_i \rangle$ decrease as

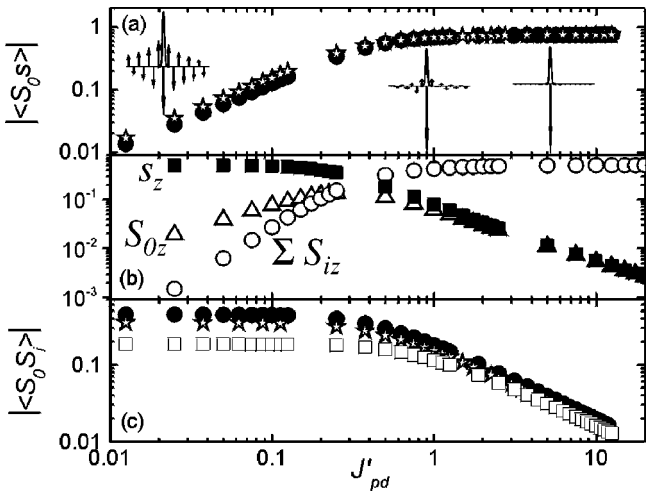

FIG. 3. (a) The correlator $|\langle \mathbf{sS}_0 \rangle|$ between the p spin and d spin on which the carrier is localized as a function of J'_{pd} for a 1D chain with PBC (filled circles) and a 2D 4×4 square with PBC (open stars). Icons show the correlators $\langle \mathbf{sS}_i \rangle$ for corresponding J'_{pd}. (b) The z component of carrier spin $\mathbf{s}_z$, of central spin $\mathbf{S}_{0z}$, and the sum of AF spins $\Sigma_i \mathbf{S}_{iz}$ are shown for an open chain of 16 spins as a function of J'_{pd}. (c) The correlator between $\mathbf{S}_0$ and its NN spin (filled circles) and NNN spin (open squares) for a chain of 16 spins. The correlator between $\mathbf{S}_0$ and its NN spin for a 2D 4×4 square with PBC is presented by stars.

J'_{pd} increases. Thus the behavior of correlators indicates the equivalence between the small polaron and nonmagnetic vacancy in a large J'_{pd} limit. Third, although the ground state of a carrier with $s = 1/2$ and an AF cluster of an even number of local spins is a spin doublet for any J'_{pd}, as it is clearly shown in Fig. 3(b), the magnetic moment is transferred from the carrier to AF spins when J'_{pd} increases. For a very strong p-d coupling $\Sigma_i S_{iz}$ saturates at 1/2. At the same time, the moments of carrier spin and of the local spin $\mathbf{S}_0$ vanish.

Thus in the limit of $J'_{pd} \gg 1$ the small polaron is equivalent to the Zhang-Rice one. Here the spins, $\mathbf{s}$ and $\mathbf{S}_0$, are compensated and form a local singlet, not coupled to other local spins, $\mathbf{S}_i$ [see Fig. 3(c) and the icon in Fig. 3(a)]. The formation of a central pair of compensated spins is accompanied by the reconstruction of AF bonds in the vicinity of the small AFP.[34] This reconstruction is driven by a gain of d-d exchange energy, and is of the order of J_{dd}. It is an important contribution to the energy of the ZR polaron for $J'_{pd} \gtrsim 1$.

To summarize, the small AFP in the range of intermediate p-d coupling (typical for high-T_c superconductors) is not equivalent to the ZR polaron. The carrier spin is also partially correlated with AF spins in the vicinity of local singlet.

D. Ferron

As it is shown in Fig. 1, E_{ex} for weak J'_{pd} strongly decreases when the charge distribution changes from a localized one in the unit cell to a homogeneous one over the entire AF cluster. Figure 2 shows that for $J'_{pd} \lesssim 1 E_{ex}$ is smaller by a factor ~ 80 for a polaron localized on two, antiferromagnetically correlated d spins, as compared to the

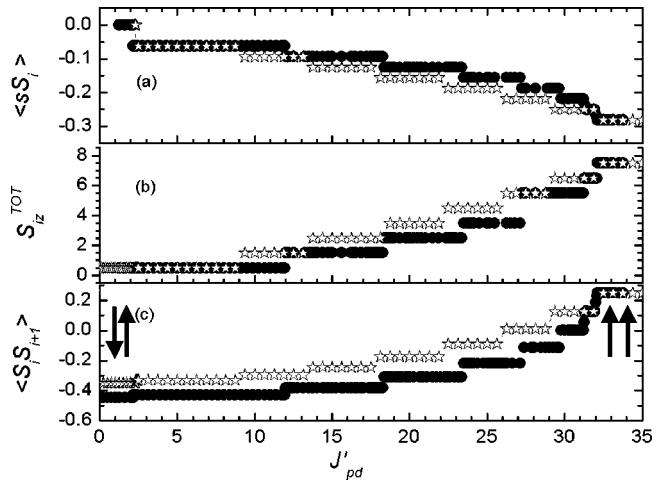

FIG. 4. (a) The correlator between the carrier spin and one of AF spin $\langle \mathbf{sS}_i \rangle$, (b) the total spin moment of the AFP polaron, S_{iz}^{tot},(c) and the correlator between NN AF spins $\langle \mathbf{S}_i \mathbf{S}_{i+1} \rangle$ as a function of J'_{pd} for evenly distributed trial function. Circles show results for a 1D chain of 16 spins with PBC while stars for the 2D 4×4 square with PBC.

case of a small AFP. For a strong $J'_{pd} \gtrsim 1$, however, an unexpected superquadratic increase of E_{ex} occurs. This effect is even stronger for a homogeneously distributed carrier density. As it is shown by squares in Fig. 2, E_{ex} for a small J'_{pd} is practically zero but sharply increases for $J'_{pd} \cong 2$ with another steplike behavior in stronger J'_{pd}. Studies of the spin structure show that this critical behavior is caused by a breakdown of the AF bonds and the formation of a magnetic moment in the AF medium. Such a magnetic polaron is known as a ferron.[32,35]

The spin structure of a ferron localized on two neighboring d spins (two spin ferron) is complex. We found that the correlator of the carrier spin **s** with the pair of local AF spins $\mathbf{S}_p$, $\langle \mathbf{sS}_p \rangle$, is negative for any antiferromagnetic J'_{pd}. For a weak J'_{pd}, $\langle \mathbf{sS}_p \rangle$ increases linearly and saturates for strong J'_{pd} at -0.5. The sharper increase of E_{ex}, which is seen for $J'_{pd} \simeq 2.5$, is caused by a spin flip of two d spins, $\mathbf{S}_p$. The systematic, faster than the linear increase of E_{ex} for $J'_{pd} \gtrsim 4$ results from a gradual reconstruction of the AF bonds around the ferron. Importantly, the value of $\langle \mathbf{sS}_p \rangle$ as well as the reconstruction of AF bonds cannot be explained in a classical approach.

More apparent data about the formation of a ferron can be found if one assumes a homogeneous distribution of the carrier on the whole AF. Figure 4 shows correlators between different spins, $\langle \mathbf{sS}_i \rangle$ and $\langle \mathbf{S}_i \mathbf{S}_{i+1} \rangle$, as well as the total magnetic moment of the polaron $\mathbf{S}_{iz}^{tot} = \Sigma_i \mathbf{S}_{iz} + \mathbf{s}_z$ as a function of J'_{pd}. The steplike behavior of all variables is clearly seen for both 1D and 2D cases. For $J'_{pd} \lesssim 2.5$ the correlators $\langle \mathbf{S}_i \mathbf{S}_{i+1} \rangle; \langle \mathbf{sS}_i \rangle = 0$ in accordance with $E_{ex} = 0$. For $J'_{pd} \gtrsim 2.5$ E_{ex} increases with the changes of correlators. Figure 4(b) shows that also $\mathbf{S}_{iz}^{tot}$ is characterized by steps occurring for the same values of J'_{pd} as those of $\langle \mathbf{sS}_i \rangle$ when $J'_{pd} \gtrsim 9$. For $J'_{pd} \lesssim 9$ and the 2D case $S_{iz}^{tot} = 1/2$. For $J'_{pd} \lesssim 2.5$ this moment is located at the carrier while for $J'_{pd} \gtrsim 2.5$ it is a result of the

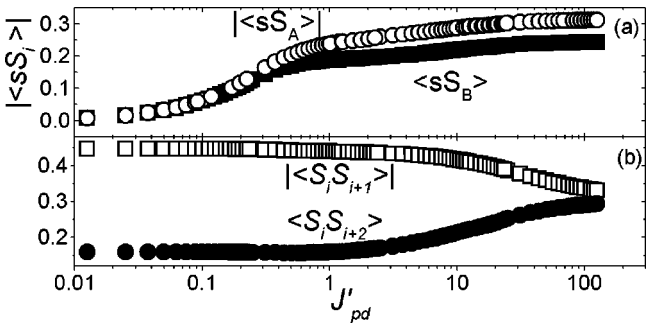

FIG. 5. (a) The mean values of the correlators $|\langle \mathbf{sS}_A \rangle|$ and $\langle \mathbf{sS}_B \rangle$ as a function of J'_{pd} for a comblike trial function. (b) The correlators $\langle \mathbf{S}_i \mathbf{S}_{i+2} \rangle$ and $|\langle \mathbf{S}_i \mathbf{S}_{i+1} \rangle|$ as a function of J'_{pd}.

coupling of the electron spin ($s_z = 1/2$) with $\Sigma_i S_{iz} = 1$ AF spin. The correlator $\langle \mathbf{S}_i \mathbf{S}_{i+1} \rangle$ changes from -0.4 for a pure AF to 1/4 (both spins parallel) as J'_{pd} increases [see Fig. 4(c)]. At the same time, S_{iz}^{tot} approaches the value 7.5 (all bonds broken). It is worth noting that the steplike behavior of $\langle \mathbf{S}_i \mathbf{S}_{i+1} \rangle$ is not a consequence of breaking of the subsequent bonds, but it is associated with steps of the total magnetic moment of the system. To summarize, the ferron can form when a homogeneous, Curie-Weiss magnetization is induced. Our results complement well the classical model.

E. Comblike AFP

A homogeneous distribution of the carrier on many d spins makes the E_{ex} on opposite spins cancel each other out. Thus we introduced a carrier trial function which is distributed on one of the Néel sublattices only as intuitively energetically favorable. The carrier distribution is described as follows: $|\varphi(i)|^2 = f(\mathbf{r}_i)\cos^2[\pi \mathbf{r}_i/(2a)]$, where $f(\mathbf{r}_i)$ is an envelope function, usually Gaussian. We call such a polaron comblike AFP.[25,33]

E_{ex} versus J'_{pd} for the comblike polaron with a Gaussian envelope function is presented by down triangles in Fig. 1. For a small r_p, the comblike AFP is equivalent to the small AFP. For a bigger r_p, the gain E_{ex} decreases, but it is still much greater than that for the large AFP. E_{ex} for a large comblike AFP is only three times smaller than that of a small AFP. This stems from a decrease of quantum fluctuations (see Sec. III F).

The comblike AFP induces a staggered magnetization in the AF medium. This is shown in Fig. 5(a), where the mean value of the correlator between the p-spin **s** and the spins of the AF sublattice on which the polaron is acting $\mathbf{S}_A$, $|\langle \mathbf{sS}_A \rangle|$, and the spins of other sublattice $\mathbf{S}_B$, $\langle \mathbf{sS}_B \rangle$, are presented. The values of the correlators increase linearly for a small $J'_{pd} \lesssim 1$, and they saturate when $J'_{pd} \gtrsim 1$ at $\langle \mathbf{sS}_B \rangle = 1/4$ for any number of d spins. The saturation value of $|\langle \mathbf{sS}_A \rangle| > 0.25$ and depends on N. The difference between the magnetization of sublattices gives the net magnetic moment of AF. This moment originates from its partial transfer from p spin to AF similar to the case of small AFP's.

The presence of the comblike AFP on one of the Néel sublattices breaks the translation symmetry and leads to the formation of two magnetized sublattices. In Fig. 5(b), the

correlators between NN's, $|\langle \mathbf{S}_i \mathbf{S}_{i+1} \rangle|$, and NNN's, $\langle \mathbf{S}_i \mathbf{S}_{i+2} \rangle$, are presented as a function of J'_{pd}. While $|\langle \mathbf{S}_i \mathbf{S}_{i+1} \rangle|$ decreases for $J'_{pd} \gtrsim 1$, the correlator $\langle \mathbf{S}_i \mathbf{S}_{i+2} \rangle$ increases. Thus a comblike AFP increases the AF correlation radius. In the limit of very large J'_{pd}, the comblike AFP transforms the quantum antiferromagnet into a classical one.

Although E_{ex} for the comblike AFP is large, its kinetic energy T is also high. Moreover, the comblike AFP has a tendency to shrink into a small AFP since T is the same for both types of polarons (as long as only t_1 is taken into account) while E_{ex} due to quantum fluctuations increases three times with localization.

F. Quantum effects

Now we summarize the results concerning different magnetic polarons. We pay particular attention to the quantum effects. In Secs. III A–E, five types of AFP's were discussed. The formation of weak small and medium as well as comblike polarons is associated with the induction of staggered magnetization. In contrast, the origin of a strong ZR polaron is the compensation of the AF spin by the carrier spin. The ferron in turn emerges due to the breaking of AF bonds, which is equivalent to the induction of a homogeneous moment.

Classically, the only mechanism of AF polaron formation at zero temperature is the alignment of the d spins by the effective field of the carrier.[32,35] However, this mechanism explains the formation of the ferron only. In contrast, staggered magnetization results directly from the quantum effects. In a quantum approach the ground state of AF is a combination of Néel states, hence no sublattice is distinguished. The simplest measure of AF quantum fluctuations is the difference between its ground and first excited state, both composed of Néel states. In the presence of the staggered field the Néel sublattices are distinguishable and the spin fluctuations are damped.[36]

Also, compensation responsible for the formation of the ZR polaron should be considered in a quantum approach. Classically, the carrier couples the AF spin leaving the AF order unchanged. As we have shown in Fig. 3(c), the quantum treatment of the AF may suppress correlations between d spins. Thus only the quantum approach allows us to model the destruction of the AF order observed in experiments.[37] Despite the quantum character of the above discussed mechanisms, there are some particular situations where the polarons can be described in the classical limit if the quantum corrections are taken into account. In particular, it is possible for strong p-d coupling. Systematic analysis of the $E_{ex}(J'_{pd})$ dependence in the range of very large J'_{pd} shows that $E_{ex} = \Sigma_i j_{pd}(i) \langle \mathbf{s}\mathbf{S}_i \rangle$, where the summation is taken over the N spins $\mathbf{S}_i$ within the polaron size (see Fig. 2). Since $\langle \mathbf{s}\mathbf{S}_i \rangle = 1/4 + 1/(2N)$, E_{ex} changes from $3/4 J'_{pd}$ for $N=1$ to $1/4 J'_{pd}$ for $N=\infty$. This makes classical calculations of E_{ex} for strong small polarons as well as ferrons possible, provided that appropriate scalar spin multiplication (1/4) is replaced by the quantum factor. It is equal to the classical value when $N \to \infty$, whereas for $N=1$ it is three times bigger. The same factor 3 is lost when the ZR polaron is spread on one of the Néel sublattices forming the comblike polaron.

The importance of the sign of the p-d coupling is shown in the inset to Fig. 2. Here E_{ex} for a small AFP with either a positive or negative J'_{pd} is presented. Different slopes of E_{ex} for ferro- and antiferromagnetic coupling are clearly seen. It stems from the fact that the carrier and AF spins cannot couple ferromagnetically to more than 1/4 while for antiferromagnetic coupling $\langle \mathbf{s}\mathbf{S}_i \rangle$ reaches $-3/4$. In the case of ferromagnetic coupling, the classical energy calculations for small polarons and ferrons are correct for strong J'_{pd} although the saturation of magnetization is much more slower in the quantum case.

G. Polaron mass

In our approach [see Eq. (2)] we assume a simple decoupling of the carrier kinetic energy T and the spin degree of freedom. For all the types of polarons discussed, the minimum energy corresponds to the localization of the carrier at the position of chosen local spin $\mathbf{r}_0$. However, another equivalent minimum corresponds to the localization at another spin site. Although our simplified approach cannot be used to study polaron dynamics, it gives a reasonable picture of the spin structure of a magnetic polaron under assumption of its static nature. Moreover, a hint about the effective polaron mass and the reduction of T can be found within our approach through the analysis of the change of the spin structure which accompanies the transfer of the polaron to the NN. Our solutions show that the spin structure of the surrounding local spins is very different when the carrier is localized on the first A or on the neighboring B site. *A posteriori*, we can claim that the matrix elements describing T are reduced by a factor resulting from the product of the spin states on the site A and B $\langle X_S^A | X_S^B \rangle$, respectively. In other words, to consider the effects which are included due to our assumption [Eq. (2)], one has to reduce the value of t_1 and consider $t_1^* = t_1 \langle X_S^A | X_S^B \rangle$. Our numerical study shows that $\langle X_S^A | X_S^B \rangle = 1$ for $J'_{pd} \ll 1$; it decreases with increasing J'_{pd}, and for $J'_{pd} \gtrsim 1$ it saturates in the range 0.1–0.2, depending on the type of polaron. It shows that the effective mass of polaron dressed by the spin polarization is considerably bigger as compared to the free one.

IV. PHASE DIAGRAM OF MAGNETIC POLARONS

So far we have considered the E_{ex} only. However, the total energy (exchange and kinetic one) should be taken into account to specify which type of magnetic polaron forms. In this section, we add kinetic energy to our consideration.

In Fig. 6 the total energy $E_{tot} = T + E_{exch}$ as a function of r_p calculated for a selected effective mass is shown for a 2D square cluster with PBC. It is seen that for $m_{eff} = m_e$ no AFP can form. For a large m_{eff} (which $\propto 1/t_1$), only small polaron can exist. The ferron does not form since J'_{pd} is too small. The medium and large polarons tend to localize in one elementary cell for any m_{eff} and t_1. This tendency to localization stems from a rapid reduction of E_{ex} with increasing r_p due to quantum fluctuations of the AF medium (see Sec.

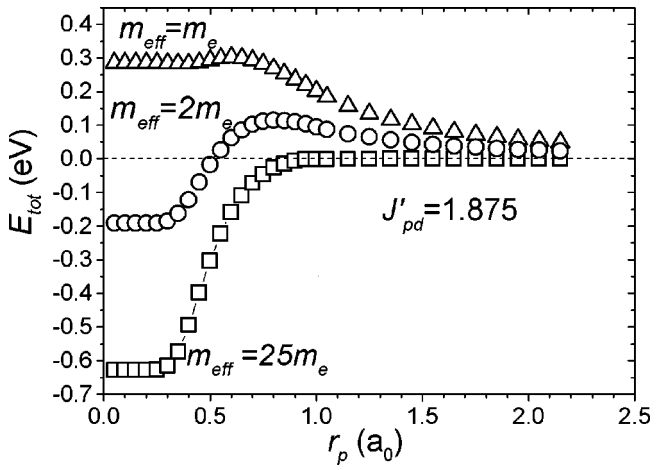

FIG. 6. E_{tot} as a function of polaron radius r_p for $J'_{pd}=1.875$ and different m_{eff}.

III F). We found that for $J'_{pd}=1.875$ magnetic polarons can form only if $m_{eff}>1.6m_e$, that is $t_1<2J_{dd}$. Also, for weaker J'_{pd} the small AFP formation is the only possibility, provided that m_{eff} is large enough.

Figure 7 shows the phase diagram of magnetic polaron formation on the t_1-J'_{pd} plane. In the inset the total energies of a small AFP and a small ferron are compared for $J'_{pd}=4.4$. E_{ex} for a small AFP is higher than for the two spin ferron, and it is constant. T of the two-spin ferron is smaller than that of a small AFP and scales linearly with t_1. Thus $E_{tot}\propto t_1$ for both polarons but with different slopes. Particularly, the boundary between the small AFP and two-spin ferron for $J'_{pd}=4.4$ crosses for $t_1=5.4J_{dd}$ when $m_{eff}=0.6m_e$. For $t_1\gtrsim 6.25J_{dd}$, neither AFP is formed. In general, the small AFP forms for $m_{eff}\gtrsim m_e$ while the two-spin ferron appears for $m_{eff}\lesssim m_e$. Similarly, we found the range of parameters for which other polarons can form.

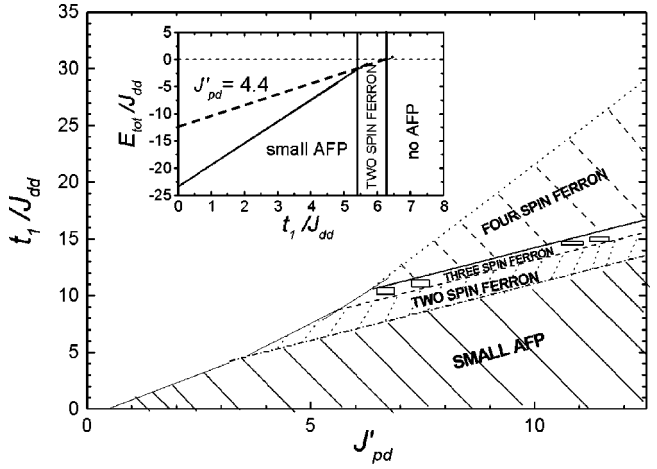

FIG. 7. Phase diagram of magnetic polaron formation. N spin ferron means ferron localized on N neighboring d spins. The inset shows E_{tot} as a function of t_1 for $J'_{pd}=4.4$. Here the dashed line presents $E_{tot}(t_1)$ for the two-spin ferron, the solid line shows $E_{tot}(t_1)$ for a small AFP. Vertical lines separate the areas of different polarons formation.

The presented results were calculated for a 2D square with PBC. To estimate the error caused by small size of the AF cluster, we studied also a 4×4 square without PBC, a 4×4 parallelogram, and $2\times N$ systems where $2\leqslant N\leqslant 10$. We find that the energy of polarons with small size depends on the nearest vicinity only. It is weakly dependent on both N and boundary conditions. For different 2D clusters, the formation range of subsequent polarons can be shifted about 10–15%.

The study of polaron formation in a wide range of parameters is exceptionally valuable to classify what type of polaron could be formed in different materials. For example, in doped EuTe where $J_{pd}\approx 0.125$ eV and $J_{dd}\approx 2$ meV,[38] the p-d coupling on one AF bonds $J'_{pd}\approx 8$. At the same time, $t_1\approx 15J_{dd}$. For such parameters, our model predicts the ferrons formation (see Fig. 7) in accord with experiments.[32,38]

In high-T_c superconductors based on CuO_2 layers, the $J_{dd}\approx 55$–75 meV as determined from the Néel temperature of AF precursors of these materials.[39] $J_{pd}\approx 1$–3 eV was determined from the band-structure calculations.[23,40–42] Thus J'_{pd} is between 1.5 and 4 for $J_{dd}=0.075$ eV. m_{eff} is much more difficult to determine because the mass observed in experiments (e.g., in ARPES) is decorated by phonon and exchange interactions. Since the decorated m_{eff} observed in ARPES experiments[43] is about $4m_e$ and m_{eff} in our model is dressed by phonons only, the m_{eff} here should be smaller than $4m_e$, which is equivalent to $t_1\gtrsim 0.8J_{dd}$.

We conclude on the basis of our phase diagram that for the parameters relevant for weakly doped high-T_c superconductors mainly the small AFP's would form. There may be also some competition between the formation of small AFP's and two-spin ferrons provided that the effective mass dressed by phonons is a bit lower than the m_e.

V. CONTRIBUTION OF PHONON AND MAGNETIC POLARON

Now we will compare the phonon and magnetic contributions to the formation of polarons in weakly doped high-T_c superconductors. We have shown that in the 2D case the small magnetic polaron forms. On the other hand, it was suggested that in high-T_c superconductors only the small phonon polaron forms and its energy is given by:[10] $E_{ph}\approx q_D e^2/(\pi\kappa)$, where $q_D=(6\pi^2/V)^{1/3}$ is the Debye momentum, $1/\kappa=1/\varepsilon-1/\varepsilon_0$; $\varepsilon,\varepsilon_0$ are dynamic and static dielectric constants, respectively, and e is the electron charge. Thus we consider here the energy of small magnetic and small phonon polarons.

Figure 8(a) shows $E_{ex}(J'_{pd})$ for a small magnetic polaron on a 2D AF square with PBC. In Fig. 8(b), the energy gain E_{ph} from the formation of phonon polaron is presented as a function of κ. Typical values of κ are between 5 and 20. The kinetic energy for both small polarons is the same, $T=4|t_1|$, and is omitted for clarity.

Horizontal and vertical dotted lines drawn in Figs. 8(a) and (b) indicate parameters $J'_{pd}=1$ and $\kappa\approx 10$ for which energy gain $E_{ex}=E_{ph}\simeq 0.35$ eV is the same for phonon and magnetic polarons. The energy gain due to the phonon po-

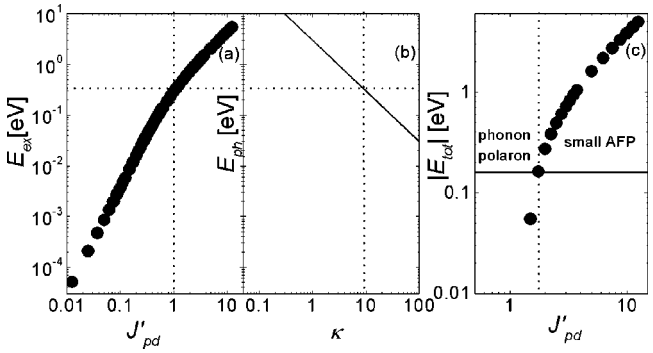

FIG. 8. (a) E_{ex} as a function of J'_{pd} for a small AFP. (b) The phonon energy E_{ph} versus κ. (c) The absolute value of the total energy for a magnetic (circles) and for a phonon (solid line) polaron as a function of J'_{pd} for $m_{eff}=2.2m_e$ and $\kappa=5$. The vertical dashed line shows the value of J'_{pd} where the magnetic and phonon polaron energies are equal.

laron is greater than that for the magnetic one for $\kappa \lesssim 10$ and $J'_{pd} \lesssim 1$. For $\kappa \gtrsim 10$ and $J'_{pd} \gtrsim 1$ the magnetic polaron dominates. One can see that for the parameters relevant for high-T_c superconductors, the energy gain from phonon and magnetic polaron is comparable, and it is of the order of fraction of eV.

Figure 8(c) presents $E_{tot}(J'_{pd})$ calculated for $m_{eff}=2.2m_e$ and $\kappa=5$[10]. This mass, according to ARPES experiments[43] and band-structure calculations,[40] is relevant for high-T_c superconductors. Since both E_{ph} and T do not depend on J'_{pd}, for the phonon polaron $E_{tot} \approx 0.15$ eV is constant. In contrast, for the magnetic polaron [circles in Fig. 8(c)] E_{tot} increases with J'_{pd}. Thus the phonon polaron dominates in the range of weak p-d couplings while the magnetic one does for strong J'_{pd}. However, in the range of $J'_{pd}=1.5$–4, which is typical for weakly doped high-T_c superconductors, the energies of both polarons are comparable or the magnetic polaron energy slightly overcomes the energy of the phonon one. This result agrees well with a very recent paper[44] which stresses the importance of phonon interactions in high-T_c superconductors. We conclude that within our model both contributions should be included in the total polaron energy for high-T_c superconductors.

VI. SUMMARY

Using the spin-fermion model and treating all spins in the quantum approach, we found that depending on the material parameters five various types of magnetic polarons in AF medium can be distinguished.

We showed that in the range of parameters typical for weakly doped high-T_c superconductors the contributions of phonon and magnetic interactions to the formation of a polaron are comparable and hybrid magnetic-phonon polarons form.

In weakly doped high-T_c superconductors small magnetic polarons as well as small ferrons can form. Our numerical study allows us to find a continuous evolution from the Zhang-Rice approach, when p-d coupling is assumed to be much stronger than d-d coupling, via the important for high-T_c materials intermediate range, to the linear-response approach suitable for weak p-d coupling.

The here considered comblike polarons cannot form when the band is empty (i.e., in undoped material) because of the high cost of kinetic energy. However, they can play a fundamental role in doped high-T_c materials when the band is partially filled.[25,33]

ACKNOWLEDGMENTS

Valuable discussion with H. Przybylińska is acknowledged. Work was supported by the KBN grant 2 P03B 007 16.

*Present address: Department of Physics and Astronomy and Ames Laboratory, Iowa State University, Ames, IA 50011.

[1] M.K. Crawford, M.N. Kunchur, W.E. Farneth, E.M. McCarron, III, and S.J. Poon, Phys. Rev. B **41**, 282 (1990).
[2] J.P. Franck, J. Jung, M.A.-K. Mohamed, S. Gygax, and G.I. Sproule, Phys. Rev. B **44**, 5318 (1991).
[3] M.R. Norman, H. Ding, M. Randeria, J.C. Campuzano, T. Yokoya, T. Takahashi, T. Mochiku, K. Kadowaki, P. Guptasarma, and D.G. Hinks, Nature (London) **392**, 157 (2000).
[4] K. Karpińska, M.Z. Cieplak, S. Guha, A. Malinowski, T. Skośkiewicz, W. Plesiewicz, M. Berkowski, B. Boyce, T.R. Lemberger, and P. Lindenfeld, Phys. Rev. Lett. **84**, 155 (2000).
[5] B.G. Levi, Phys. Today **17** (3), 53 (2000).
[6] C. Castellani, C. DiCastro, and M. Grilli, Phys. Rev. Lett. **75**, 4650 (1995).
[7] S.I. Pekar, Zh. Eksp. Teor. Fiz. **16**, 335 (1951).
[8] H. Fröhlich, Phys. Rev. **79**, 845 (1954).
[9] H. Fröhlich, Adv. Phys. **3**, 325 (1954).
[10] A. S. Alexandrov and N. Mott, *Polarons and Bipolarons* (World Scientific, Singapore, 1995).
[11] A.S. Alexandrov, Phys. Rev. B **38**, 925 (1988).
[12] A.J. Millis, H. Monien, and D. Pines, Phys. Rev. B **42**, 167 (1990).
[13] F.C. Zhang and T.M. Rice, Phys. Rev. B **37**, 3759 (1988).
[14] E. Dagotto, Rev. Mod. Phys. **66**, 763 (1994).
[15] S.R. White and D.J. Scalapino, Phys. Rev. Lett. **84**, 3021 (2000).
[16] C.S. Hellberg and E. Manousakis, Phys. Rev. Lett. **84**, 3022 (2000).
[17] S. Schmitt-Rink, C.M. Varma, and A.E. Ruckenstein, Phys. Rev. Lett. **60**, 2793 (1988).
[18] C.L. Kane, P.A. Lee, and N. Read, Phys. Rev. B **39**, 6880 (1989).
[19] V. Elser, D.A. Huse, B.I. Shraiman, and E.D. Siggia, Phys. Rev. B **41**, 6715 (1990).
[20] A. Ramsak and P. Horsch, Phys. Rev. B **48**, 10559 (1993).
[21] G.F. Reiter, Phys. Rev. B **49**, 1536 (1994).
[22] Z. Liu and E. Manousakis, Phys. Rev. B **45**, 2425 (1992).
[23] C. Buhler, S. Yunoki, and A. Moreo, Phys. Rev. Lett. **84**, 2690 (2000).
[24] B.L. Altshuler, L.B. Ioffe, and A.J. Millis, Phys. Rev. B **52**, 5563 (1995).
[25] E.M. Hankiewicz, R. Buczko, and Z. Wilamowski, Physica B **284-288**, 437 (2000).

[26] J.R. Schrieffer, J. Low Temp. Phys. **99**, 397 (1995).
[27] A. Ramsak and P. Prelovsek, Phys. Rev. B **42**, 10415 (1990).
[28] M. Hamada and H. Shimahara, Phys. Rev. B **51**, 3027 (1995).
[29] J. Ba̋la, A.M. Oleś, and J. Zaanen, Phys. Rev. B **54**, 10 161 (1996).
[30] J. Ba̋la and A.M. Oleś, Phys. Rev. B **61**, 6907 (2000).
[31] J.J.M. Pothuizen, R. Eder, N.T. Hien, M. Matoba, A.A. Menovsky, and G.A. Sawatzky, Phys. Rev. Lett. **78**, 717 (1997).
[32] T. Kasuya and A. Yanase, Rev. Mod. Phys. **40**, 684 (1968).
[33] E.M. Hankiewicz, R. Buczko, and Z. Wilamowski, Acta Phys. Pol. A **97**, 185 (2000).
[34] M. Laukamp, G.B. Martins, C. Gazza, A.L. Malvezzi, E. Dagotto, P.M. Hansen, A.C. Lopez, and J. Riera, Phys. Rev. B **57**, 10 755 (1998).
[35] V.D. Lakhno and E. Nagaev, Fiz. Tverd. Tela (Leningrad) **18**, 3429 (1976) [Sov. Phys. Solid State **18**, 1995 (1976)].
[36] Z. Wilamowski and E.M. Hankiewicz, Acta Phys. Pol. A **97**, 403 (2000).
[37] R.J. Birgeneau, D.R. Gabbe, H.P. Jenssen, M.A. Kastner, P.J. Picone, T.R. Thurston, G. Shirane, Y. Endoh, M. Sato, K. Yamada, Y. Hidaka, M. Oda, Y. Enomoto, M. Suzuki, and T. Murakami, Phys. Rev. B **38**, 6614 (1988).
[38] P. Wachter, in *Handbook on the Physics and Chemistry of the Rare Earths*, edited by K. A. Geschneider, Jr. and L. Eyring (North-Holland, Amsterdam, 1979), Vol. 2, p. 507.
[39] N. M. Plakida, *High Temperature Superconductivity* (Springer-Verlag, Berlin, 1995).
[40] M.S. Hybertsen, E.B. Stechel, M. Schluter, and D.R. Jennison, Phys. Rev. B **41**, 11 068 (1990).
[41] H. Eskes, L.H. Tjeng, and G.A. Sawatzky, Phys. Rev. B **41**, 288 (1990).
[42] C.X. Chen, H.B. Schüttler, and A.J. Fedro, Phys. Rev. B **41**, 2581 (1990).
[43] G. Mante, R. Claessen, T. Buslaps, S. Harmand, R. Manzke, and M.S.J. Fink, Z. Phys. B: Condens. Matter **80**, 181 (1990).
[44] A. Lanzara, P.V. Bogdanov, X.J. Zhou, S.A. Kellar, D.L. Feng, E.D. Lu, T. Yoshida, H. Eisaki, A. Fujimori, K. Kishio, J.-I. Shimoyama, T. Noda, S. Uchida, Z. Hussain, and Z.-X. Shen, Nature (London) **412**, 510 (2001).